DEWATERING STRESS ADJUSTMENT AND EFFECT ON MINING PRESSURE IN DEEP SANDSTONE ROOF

by

***Shuang YOU*[a,b], *Qian-Cheng GENG*[a,b*], *Hong-Guang JI*[a,b], *and Long-Long ZHAO*[a,b]**

[a] School of Civil and Resources Engineering,
University of Science and Technology Beijing, Beijing, China
[b] Beijing Key Laboratory of Urban Underground Space Engineering, USTB, Beijing, China

Original scientific paper
https://doi.org/10.2298/TSCI2502137Y

To explore the coupling relationship between stress field adjustment and mining pressure in the sandstone roof at great depth under dewatering conditions, a mechanical linkage mathematical model based on elastic theory was constructed to estimate the stress adjustment in the dewatering area and its interaction with mining pressure. Additionally, the Sobol global sensitivity analysis method was introduced to evaluate the importance and interaction of various factors affecting the stress adjustment in the roof area. The study found that the main factors influencing the vertical stress at point M, in order of significance, are the horizontal distance from point M to the dewatering outlet, the pressure head of the aquifer at the dewatering outlet, the permeability coefficient of the dewatering stratum, and the influence coefficient of dewatering; among these, a significant interaction exists between the horizontal distance from point M to the dewatering outlet and the pressure head of the aquifer at the dewatering outlet, while interactions among other parameters are less significant or negligible.

Key words*: mining pressure, dtress adjustment, mathematical model, sensitivity analysis, Sobol analysis*

Introduction

With the increasing depth of mining resource extraction, the burial depth of mines is rising, and the stability of roof rock layers has become a key issue for mine safety [1, 2]. Especially under conditions of great burial depth, dewatering of groundwater can trigger the redistribution of the regional stress field [3], thereby affecting the evolution of mining pressure in the working face.

At present, extensive research has been conducted on the coupling relationship between stress field adjustment and mining pressure under deep burial roof dewatering conditions [4-6]. Song *et al*. [7] revealed the theoretical mechanism of groundwater inflow at the coal seam floor above a confined aquifer. Huang *et al*. [8] derived a transfer matrix in the transform domain that describes the relationship between mining pressure and stress at any depth in multilayer rock formations. Shu *et al.* [9] demonstrated that dewatering causes heterogeneous damage to the physical and mechanical parameters of the aquifer, leading to local stress concentration in the coal seam. Tzampoglou *et al*. [10] analyzed the reduction in pore pressure and the corresponding increase in effective stress within the strata. Xu *et al*. [11] analyzed the load

* Corresponding author, e-mail: gqch0109@163.com

transfer function of loose confined aquifers and the development characteristics of water-conducting fractures in coal roof rock, as well as the mechanism of water inrush.However, most of the existing research focuses on the influence of single factors, such as changes in water pressure or localized analysis of stress adjustment, lacking a systematic analysis of the interlinking mechanisms.

This paper aims to construct a linkage mechanism model of regional stress field adjustment of roof dewatering and ground pressure in the mining area under the condition of great burial depth, analyze the dynamic process of the influence of groundwater dewatering on ground pressure change and roof stability, and provide theoretical basis and technical support for the safe mining of deep mines.

Analysis of support pressure patterns under dewatering

The self-weight stress of the roof rock layers and groundwater pressure jointly act on the rock mass. When dewatering reduces the groundwater level, the rock layers previously supported by water pressure lose their support, leading to stress concentration phenomena. This adjustment of the stress field is not only evident in the dewatering area but also affects the stress distribution in surrounding regions, fig. 1. For simplification of calculations, the main impact area of dewatering is approximated as an isosceles trapezoid with the dewatering hole at the bottom center, a height equal to the aquifer height, h_{1i}, a lower base, $2R_{max}$, and an upper base, R_{max}. The coal seam roof belt is selected as the study subject. A cross-sectional diagram along the working face is drawn, assuming the rock mass is infinite and the ground is horizontal, with the origin O at the center of the dewatering hole. A corresponding mathematical model for stress transfer due to dewatering is established.

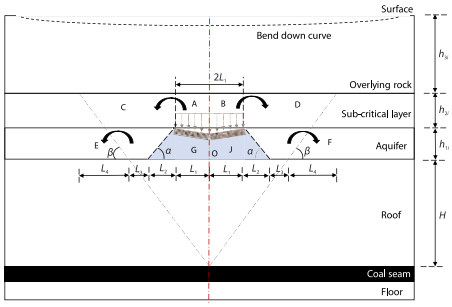

Figure 1. Analysis of the stress environment for roof support pressure after dewatering

The rock structural damage caused by dewatering lead to a reduction in the support pressure on the overlying rock layers A and B in the main affected area of dewatering. Consequently, the reactive support force on the overlying rock layers by the main affected area after dewatering is expressed:

$$\sigma_1 = k\gamma_{2i}h_{2i} + \gamma_{3i}h_{3i} - p_w \tag{1}$$

where σ_1 is the adjust stress, k – the dewatering influence coefficient, γ_{2i}, γ_{3i} are the corresponding rock bulk densities, h_{2i}, h_{3i} are the corresponding rock thickness, and p_w – the water pressure reduction.

The dewatering disturbance leads to varying settling rates among rock layers, causing delamination and load transfer. The loads from rock layers A and B transfer to layers C and D, which in turn transfer their loads to layers E and F, eventually creating a stable structure. The transferred load, Q_{AB}, from layers A and B is evenly distributed to layers C and D as Q_A and Q_B. There are:

$$Q_A = \frac{Q_{AB}}{2} = (1-k)\gamma_{2i}h_{2i}L_1 + 2p_wL_1, \quad L_1 = \frac{R_{max}}{2} = 5\frac{p_w}{\gamma_w}\sqrt{K_s} \tag{2}$$

where L_1 is the corresponding length in the mechanical model, γ_w – the bulk density of water, and K_s – the rock permeability coefficient.

The horizontal disturbance of the rock layers C and D due to dewatering is considered negligible. The load stress transferred, Q_A, from region A to region C is distributed in the form of a right triangle. The loads transferred from region C to both sides, denoted as Q_{CE} and Q_{CG}, can be represented:

$$Q_{CE} = \frac{L_4(\gamma_{2i}h_{2i} + \gamma_{1i}h_{1i})}{2} + \frac{L_4^2 Q_A}{2\sum_{i=3}^{4} L_i \sum_{i=2}^{4} L_i} \tag{3}$$

where L_i is the corresponding length in the mechanical model.

After the load from rock layer C is transferred to rock layer E, the stress distribution is approximately an isosceles triangular distribution, which can be expressed:

$$\sigma_{CE} = \frac{2Q_{CE}\tan\beta}{h_{1i} + h_{2i}} \tag{4}$$

where, σ_{CE} s the transfer stress and β – the dewatering overburden movement angle.

Based on continuum mechanics and the laws of stress transfer, the distribution function, $\sigma_w(x_i)$, for the support pressure of the roof under dewatering is shown:

$$\sigma_w(x_1) = \begin{cases} \gamma_{1i}h_{1i} + k\gamma_{2i}h_{2i} + \gamma_{3i}h_{3i} - p_w, [0, L_1) \\ \dfrac{\left(Q_A + \gamma_{2i}h_{2i}\sum_{i=1}^{4} L_i\right)(x_2 - L_1) + (k\gamma_{2i}h_{2i} - \Delta p_w)(L_1 + L_2 - x_2)\sum_{i=1}^{4} L_i}{L_2\sum_{i=1}^{4} L_i} + \gamma_{1i}h_{1i} + \gamma_{3i}h_{3i}, [L_1, L_1 + L_2) \\ \gamma_i h_i + \dfrac{\left(\sum_{i=1}^{4} L_i - x_2\right)Q_A}{(L_3 + L_4)\sum_{i=1}^{4} L_i}, [L_1 + L_2, L_1 + L_2 + L_3) \\ \gamma_i h_i + \dfrac{\left(\sum_{i=1}^{4} L_i - x_2\right)Q_A}{(L_3 + L_4)\sum_{i=1}^{4} L_i} + \dfrac{2\sigma_{CE}\left(x_2 - \sum_{i=1}^{3} L_i\right)}{L_4}, \left[L_1 + L_2 + L_3, \dfrac{2L_1 + 2L_2 + 2L_3 + L_4}{2}\right) \\ \gamma_i h_i + \dfrac{\left(\sum_{i=1}^{4} L_i - x_2\right)Q_A}{(L_3 + L_4)\sum_{i=1}^{4} L_i} + \dfrac{2\sigma_{CE}\left(\sum_{i=1}^{4} L_i - x_2\right)}{L_4}, \left[\dfrac{2L_1 + 2L_2 + 2L_3 + L_4}{2}, L_1 + L_2 + L_3 + L_4\right) \\ \gamma_i h_i, [L_1 + L_2 + L_3 + L_4, +\infty) \end{cases} \tag{5}$$

where x_1 is the distance from the stress point to the center of the dewatering roadway and γ_i – the the bulk density of the corresponding rock layer.

Dynamic model of stress adjustment and mining pressure interlinkage in dewatering areas

As the working face advances, the coal body in front of the mining area not only bears the load of the overlying rock layer, but also bears the load of the overlying rock layer in the goaf transmitted through the hanging roof effect of the broken zone rock layer. This synthetic

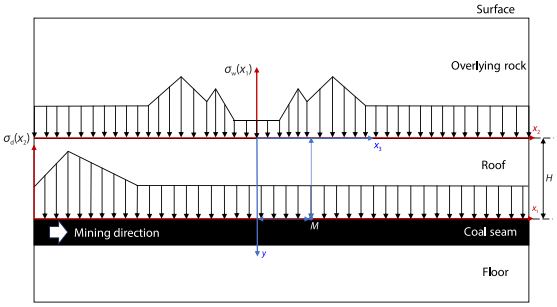

Figure 2. Dynamic model of dewatering and mining disturbance interlinkage for deeply buried roofs

stress may increase the risk of rock burst. In order to analyze the interaction between precipitation stress adjustment and mining pressure, the roof belt is studied, as shown in fig. 2. Using elastic theory to analyze the stress of a semi-infinite body under the action of distributed force, the stress component of any point in the plane can be calculated:

$$\sigma_c(x_3) = -\frac{2}{\pi}\int_{-b}^{a}\frac{[\sigma_w(\xi)-q]H^3 \mathrm{d}\xi}{\left[H^2+(x_3-\xi)^2\right]^2} \tag{6}$$

where x_3 is the vertical distance from stress point M to the center of the dewatering area, H – the thickness of the roof, and q – the self-weight stress.

Equation (6) shows that the stress component at any point in the plane is inversely proportional to x_3, meaning the further the point is from the upper distributed force, the less it is affected. When the horizontal distance between the point and the force reaches $3(a + b + H)$, the impact is reduced to 10^{-2}. Therefore, beyond this range, the dehydration effect is ignored. When an aquifer lies above the coal seam, there are two typical scenarios:

– outside the dewatering range, affected by self-weight stress and advanced support pressure and
– within the dewatering range, affected by self-weight stress, dewatering, and advanced support pressure. The vertical stress, σ_M, at point M in the coal seam can be approximated:

$$\sigma_M(x) = \begin{cases} \sigma_d(x_2), x \in [3(a+b+H), +\infty) \\ \sigma_d(x_2) + \sigma_c(x), x \in [0, 3(a+b+H)) \end{cases} \tag{7}$$

where x_3 is the vertical distance from stress point M to the center of the dewatering area and x – the horizontal distance.

Model validation and parameter sensitivity analysis

The interlinking dynamics model integrates stress adjustments in the dewatering area with changes in mining pressure for more accurate analysis. To explore its engineering applicability, the 1303 working face of a kilometer-level coal mine in Shandong was selected for study. Calculations focused on the dewatering disturbance and excavation stress fields above the coal seam. According to the hydrogeological report, with a burial depth between 933 m and 1035 m. The working face is 240 m long. The Lower Shih-box group aquifer, 25 m above the roof, is 38 m thick with a confining pressure head of 8 MPa. Based on the rock mechanics parameters and strata information, substituting them into eqs. (1)-(7) yields a stress concentration of 2.03 MPa near the cut-eye by the dewatering well due to dewatering, while the on-site monitoring result is 2.18 MPa, a difference of 6.88%. During the retreat mining process, when mining reaches 35 m away from the dewatering well, the support pressure at the working face peaks at a calculated value of 39.82 MPa, compared to the on-site monitoring result of 39.27 MPa, differing by only 1.38%. This fully demonstrates that the interlinking model has a high degree of congruence with on-site monitoring results and can effectively and accurately predict changes in mining pressure. Therefore, this interlinking dynamics model has high engineering applicability in predicting mining pressure in deep buried roof dewatering areas.

In the parameter sensitivity analysis, the horizontal distance, x, between point M and the dewatering outlet, the pressure head, p_w, between the dewatering outlet and the aquifer, the dewatering influence coefficient, k, and the permeability coefficient, K_s, of the dewatering stratum are selected for sensitivity analysis. The calculations assume the horizontal distance, x_1, from point M to the coal face is zero. The sensitivity ranking of all model parameters on the vertical stress at point M is, in order: x, p_w, K_s, and k. The sensitivity of k is the smallest, and its main and total effects are almost negligible compared to the other three parameters. Therefore, the influence of k on the vertical stress at point M is disregarded. Setting the horizontal distance x_1 to 0 and k to 0.5, the Sobol analysis is used to analyze the direct and indirect effects of the remaining three variables on the vertical stress at point M, as shown in fig. 3.

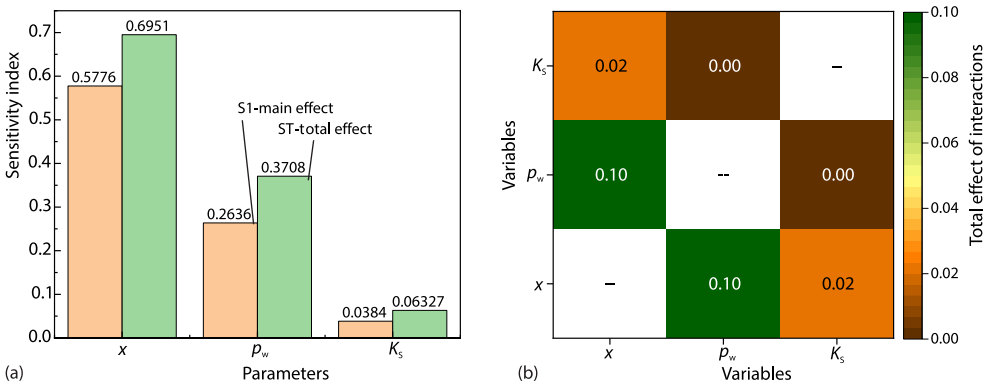

Figure 3. Sensitivity analysis of x, p_w, and K_s; (a) main effect and total effect analysis and (b) bivariate interaction effect analysis

Figure 3 shows the main effects of x, p_w, and K_s on the vertical stress at point M as 0.582, 0.258, and 0.044, respectively. The horizontal distance, x, has the largest impact, significantly affecting water pressure propagation and vertical stress. While the effect of p_w is smaller, as the pressure head influences dewatering efficiency and the surrounding pressure. Although the effect of K_s is only 0.044, it still affects water flow through the rock layers and should not be ignored. The total effects of x, p_w, and K_s on the vertical stress at point M are 0.695, 0.371, and 0.063, all greater than their corresponding main effects. This suggests that x not only has a direct effect on the vertical stress at point M but also produces an indirect effect through interactions with p_w and K_s. The total effects of p_w and K_s also indicate the presence of interactions. To further analyze the interactions between these parameters, the total effect of the bivariate combinations is used to measure the interaction between two variables. The total effects of the bivariate combinations x and p_w, x and K_s, and p_w and K_s are 0.1, 0.02, and 0. This indicates that there is a significant interaction between x and p_w regarding the vertical stress response at point M, while the interactions between x and K_s and between p_w and K_s are less significant or absent. Specifically, x and p_w exhibit a relatively high total effect in their bivariate combination, this higher interaction effect could be because the water pressure changes are directly affected by both the pressure head and the distance to the dewatering outlet. The bivariate combination of x and K_s has a lower total effect, indicating that while the interaction between x and K_s does influence the output, this influence is relatively small. This suggests that the combined effect of the horizontal distance from the dewatering outlet and the permeability coefficient of the dewatering stratum on vertical stress is not very critical, or that the interaction between these two variables is relatively minor compared to their individual main effects. The total effect of

zero for the bivariate combination of p_w and K_s indicates that there is no significant interaction between the pressure head at the dewatering outlet and the permeability coefficient of the dewatering stratum in influencing vertical stress. This may imply that these two parameters have relatively independent effects on vertical stress. Therefore, when considering dewatering strategies and strata management, special attention should be given to the joint adjustment of x and p_w, as their interaction could lead to significant changes in vertical stress.

Conclusion

Given the effects of hydraulic pressure drop gradient, dewatering level, and rock strata permeability on deep sandstone roof, a mathematical model of the mining pressure adjusted with dewatering stress was established. The theoretical prediction results showed an error rate of 1.38% compared to on-site monitoring results. Model parameters ranked by sensitivity to vertical stress at point M are (from highest to lowest): x, p_w, K_s, and k.

Acknowledgment

This work was supported by the Deep Earth Probe and Mineral Resources Exploration-National Science and Technology Major Projec (Grant No. 2024ZD1004103), the National Key Research and Development Program of China (Grant No. 2023YFC2907403), the National Natural Science Foundation of China (Grant No. 52074021), the Beijing Natural Science Foundation (Grant No. 2242045).

Nomenclature

q – self-weight stress, [MPa]
x – horizontal distance, [m]

Greek symbols

β – dewatering overburden movement angle, [°]
$\sigma_c(x_3)$ – stress at any point within the plane, [MPa]
$\sigma_M(x)$ – vertical stress, [MPa]
$\sigma_w(x_i)$ – distribution function, [MPa]

References

[1] Yang, M. Q., *et al*., Experimental Study on Non-Linear Mechanical Behavior and Sampling Damage Characteristics of Rocks from Depths of 4900-6830 m in Well Songke-2, *Journal of Central South University*, *30* (2023), 4, pp. 1296-1310
[2] Geng, Q. C., *et al*., Correlation between Micro-Structure and Acoustic Emission Characteristics of Granite by Split Tests, *Thermal Science*, *27* (2023), 1B, pp. 663-670
[3] Qiao, W., *et al*., Characteristic of Water Chemistry and Hydrodynamics of Deep Karst and Its Influence on Deep Coal Mining, *Arabian Journal of Geosciences*, *7* (2014), 4, pp. 1261-1275
[4] Bukowski, P., Water Hazard Assessment in Active Shafts in Upper Silesian Coal Basin Mines, Mine Water *and the Environment*, *30* (2011), 4, pp. 302-311
[5] Shi, L., *et al.*, Evaluation of Water Inrush from Underlying Aquifers by Using A Modified Water-Inrush Coefficient Model and Water-Inrush Index Model: A Case Study in Feicheng Coalfield, China, *Hydrogeology Journal*, *27* (2019), 6, pp. 2105-2119
[6] Wang, J. C., *et al*., Mechanism of Rock Burst Occurrence in Specially Thick Coal Seam with ROCK Parting, *Rock Mechanics and Rock Engineering*, *49* (2016), 5, pp. 1953-1965
[7] Song, W., *et al*., Theoretical and Numerical Investigations on Mining-induced Fault Activation and Groundwater Outburst of Coal Seam Floor, *Bulletin of Engineering Geology and the Environment*, *80* (2021), 7, pp. 1-12
[8] Huang, Q., *et al*., Analytical Model of Stress Field and Failure Depth in Multilayered Rock Masses of Mining Floor Based on the Transfer Matrix Method, *Geotechnical and Geological Engineering*, *35* (2017), 6, pp. 2781-2788
[9] Shu, C. X., *et al.*, Mechanism and Treatment of Rock Burst Induced by Dewatering in Roadways in Deep Coal Mines, *Journal of Mining & Safety Engineering*, *35* (2018), 4, pp. 780-786

[10] Tzampoglou, P., *et al*., Evaluating Geological and Geotechnical Data for the Study of Land Subsidence Phenomena at the Perimeter of the Amyntaio Coalmine, Greece, *International Journal of Mining Science and Technology*, *28* (2018), 4, pp. 601-612
[11] Xu, J. L., *et al*., Study on Water-inrush Mechanism and Prevention during Coal Mining under Unconsolidated Confined Aquifer, *Journal of Chian Coal Society*, *28* (2011), 3, pp. 333-339

Paper submitted: July 16, 2024
Paper revised: October 5, 2024
Paper accepted: November 23, 2024